Experimental and Theoretical Study of the Effect of Active-Site Constrained Substrate Motion on the Magnitude of the Observed Intramolecular Isotope Effect for the P450 101 Catalyzed Benzylic Hydroxylation of Isomeric Xylenes and 4,4′-Dimethylbiphenyl

Christian Audergon,[†] Krishna R. Iyer,[†] Jeffrey P. Jones,*[,‡] John F. Darbyshire,[†] and William F. Trager*[,†]

Contribution from the Department of Medicinal Chemistry, School of Pharmacy, University of Washington, Seattle, Washington 98195, and Department of Chemistry, Washington State University, Pullman, Washington 99164

Received August 20, 1998

Abstract: The validity of a cytochrome P450 (P450) 101 force field developed previously was tested by comparing to published results from other laboratories the predicted regioselectivity and stereoselectivity of both (*R*)- and (*S*)-norcamphor oxidation when the force field was used. Once validated, the force field was used to test the hypothesis that the magnitude of an observed intramolecular isotope effect is a function of the distance between equivalent but isotopically distinct intramolecular sites of oxidative attack. Molecular dynamics simulations and kinetic deuterium isotope effect experiments on benzylic hydroxylation were then conducted for a series of selectively deuterated isomeric xylenes and 4,4′-dimethylbiphenyl with P450 101. The molecular dynamics simulations predicted that the rank order of substrate mobility in the active site of P450 101 was *o*-xylene > *p*-xylene > dimethylbiphenyl. The observed isotope effects for the trideutero analogues were 10.6, 7.4, and 2.7, for the *o*-xylene, *p*-xylene, and 4,4′-dimethylbiphenyl, respectively. Thus, as the theoretically predicted rates of interchange between the isotopically distinct methyl groups decrease, the observed isotope effect decreases. The agreement between the theoretical predictions and experimental results provides strong support for the distance hypothesis stated above and for the potential of computational analysis to enhance our understanding of protein/small molecule interactions.

Introduction

The P450s are a superfamily of enzymes that utilize molecular oxygen to catalyze the oxidation of organic compounds of diverse structure. The importance of understanding their catalytic and structural properties is underscored by their presence in virtually all living organisms and their ability to metabolize essentially any organic compound to which they are exposed. An X-ray structure can be particularly valuable in elucidating the properties of an enzyme by providing a structural foundation for understanding its catalytic behavior. Once the atomic coordinates are available, computer-driven modeling studies can be used to probe enzyme properties that are not readily accessible experimentally. For many enzyme and receptor systems, computational approaches[1−4] including pattern recognition,[5] pharmacophore modeling,[6,7] comparative molecular field analysis,[8] and molecular dynamics simulations[9] have proven to be enormously valuable both in the design of new drugs (agonists or antagonists) and the establishment of predictive models for metabolism and toxicity. Similar progress for the mammalian forms of P450 has been impeded because X-ray crystallographic structures for these membrane-bound enzymes are not available.

In the absence of crystal structures, insight into structural aspects of this class of enzymes has necessitated the use of indirect approaches. Such approaches have included homology modeling of unknown structures based on the few soluble prokaryote forms of the enzyme for which X-ray structures are available, site directed mutagenesis, attempts at active-site mapping with mechanism-based inhibitors, and kinetic isotope effects. Previous studies have established that the magnitude of an observed intramolecular deuterium isotope effect, $(k_H/k_D)_{obs}$, is highly dependent upon a rapid rate of equilibration, relative to the actual bond-breaking event, between the chemically equivalent but isotopically distinct protio and deutero metabolic sites in the substrate, with respect to a catalytically susceptible orientation.[10−12] If equilibration is rapid, the observed

[†] University of Washington.
[‡] Washington State University.

(1) Nemethy, G.; Scheraga, H. A. *FASEB J.* **1990**, *4*, 3189−3197.
(2) Sun, E.; Cohen, F. E. *Gene* **1993**, *137*, 127−132.
(3) Sezerman, U.; Vajda, S.; Cornette, J.; DeLisi, C. *Protein Sci.* **1993**, *2*, 1827−1843.
(4) Loew, G. H.; Villar, H. O.; Alkorta, I. *Pharm. Res.* **1993**, *10*, 475−486.
(5) Kirschner, G.; Kowalski, B. In *Drug Design*; Ariens, E. J., Ed.; Academic Press: New York, 1979; pp 73−131.
(6) Mayer, D.; Naylor, C. B.; Motoc, I.; Marshall, G. R. *J. Comput.-Aided Mol. Des.* **1987**, *1*, 3−16.
(7) Wang, S.; Milne, G. W. A.; Yan, X.; Posey, I. J.; Nicklaus, M. C.; Graham, L.; Rice, W. G. *J. Med. Chem.* **1996**, *39*, 2047−2054.
(8) Cramer, R. D., III; Patterson, D. E.; Bunce, J. D. *Prog. Clin. Biol. Res.* **1988**, *291*, 161−165.
(9) Karplus, M.; Petsko, G. A. *Nature* **1990**, *347*, 631−639.
(10) Jones, J. P.; Korzekwa, K. R.; Rettie, A. E.; Trager, W. F. *J. Am. Chem. Soc.* **1986**, *108*, 7074−7078.
(11) Jones, J. P.; Trager, W. F. *J. Am. Chem. Soc.* **1987**, *109*, 2171−2173.
(12) Jones, J. P.; Korzekwa, K. R.; Rettie, A. E.; Trager, W. F. *J. Am. Chem. Soc.* **1988**, *110*, 2018. (Additions and Corrections.)

10.1021/ja983000w CCC: $18.00
Published on Web 12/16/1998

isotope effect $(k_H/k_D)_{obs}$ is equal to the intrinsic isotope effect (k_H/k_D) for the reaction.[13−17] If the equilibration rate is slow, or of the same order of magnitude as bond breaking, $(k_H/k_D)_{obs}$ will vary between a value of 1 (no isotope effect) and k_H/k_D (maximum (intrinsic) isotope effect). Factors that can affect equilibration rate can affect the magnitude of $(k_H/k_D)_{obs}$.[18] These factors are termed masking factors, and include slow dissociation of the enzyme−substrate complex and restrictions on reorientation of substrate in the active site. Thus, the value of $(k_H/k_D)_{obs}$ and the extent of its departure from k_H/k_D has the capacity to provide unique information on substrate motion in the active site.

Previous isotope effect studies indicate that the intrinsic isotope effects for cytochrome P450 catalyzed hydroxylations of methyl groups in different electronic environments are relatively insensitive to changes in enzyme active site architecture.[19,20] While differences in substrate electronic character may dictate different intrinsic isotope effects for the methyl group hydroxylation of a saturated hydrocarbon versus that of the *N*-methyl of an aromatic amine, the intrinsic isotope effect for the methyl group hydroxylation of a given substrate is essentially invariant across different P450 isoforms that are capable of catalyzing the reaction. This insensitivity further suggests that any significant departure of $(k_H/k_D)_{obs}$ from k_H/k_D, for the same or similar substrates, is not due to changes in energetics or mechanism but rather to factors that are capable of masking k_H/k_D. Likely factors are the distance between chemically equivalent but isotopically distinct catalytic sites in the substrate and/or active site constraint of substrate motion. To test the hypothesis that distance is the factor that can affect the magnitude of $(k_H/k_D)_{obs}$, a set of substrates was chosen in which this distance between the catalytic sites was systematically varied. The chosen substrates included selectivity deuterated *o*-xylene, *p*-xylene, and 4,4′-dimethylbiphenyl where the distance between carbon atoms of equivalent protio and deutero sites is geometrically fixed for each substrate but varies from a minimum of 2.48 Å (*o*-xylene) to a maximum of 11.05 Å (4,4′-dimethylbiphenyl)[21] between substrates,[18] Figure 1. The fixed distances and the lack of orienting elements such as polar- or hydrogen-bonding sites allowed the combination of the effects of distance and active-site constraints to be explored without the complication of additional contributing features. The results of this study strongly suggested that the near complete suppression of k_H/k_D for the benzylic hydroxylation of 4-$^2H_3$,4′-dimethylbiphenyl, whether catalyzed by P450 2B1 or various microsomal preparations, was a direct consequence of the 11.05 Å distance separating the carbon atoms of the 4 and 4′ methyl groups.

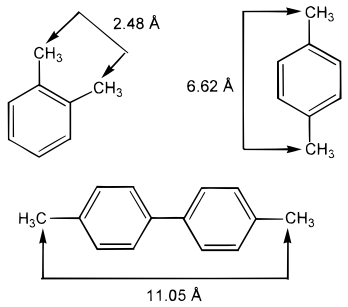

Figure 1. Intramolecular distances between methyl group carbon atoms for *o*- and *p*-xylene and 4,4′-dimethylbiphenyl calculated using Spartan Molecular Mechanics software.

Although the earlier study[18] suggested that intrinsic isotope effect masking and distance are related, it did not have the capacity to reveal the exact cause of masking or the relative rates of dissociation and active site reorientation for each substrate. In contrast, molecular dynamics simulations could provide validation of the distance/constrained motion hypothesis since such studies would allow direct assessment of the mobility of a substrate in the active site of a P450 of known crystal structure and one for which the atomic coordinates are readily available. Indeed, molecular dynamics computational studies have been used to determine active-site motions in enzymes such as triosephosphate isomerase,[22] ribonuclease T1,[23] and carboxypeptidase A.[24] In the case of P450, the bacterial isoform P450 101 has been studied extensively by using substrate-bound models originating from known X-ray crystal data, e.g., camphor, norcamphor, and thiocamphor,[25−28] whereas other studies have adapted these models to study valproic acid, benzo[*a*]pyrene, and nicotine in the enzyme−substrate complex.[29−31] Overall, these studies have led to a greater understanding of active-site architecture, substrate-binding phenomena, and catalytically related motion of both substrate and enzyme.

In this paper, we present results from parallel experimental and computational studies that provide strong support for the hypothesis that the degree of masking found in intramolecular isotope effects is directly related to the rates of interchange between chemically equivalent but isotopically distinct metabolic sites in the active site. This methodology provides a means of assessing the constraints of an enzyme active site toward substrate motion. Furthermore, these experiments provide insight into how to approach synchronization of experimental and molecular dynamics clocks.

Results

Validation of the Molecular Dynamics Protocols with D-(1*R*)- and L-(1*S*)-Norcamphor. The relative carbon radical

(13) Northrop, D. B. *Biochemistry* **1975**, *14*, 2644−2651.
(14) Northrop, D. B. In *Isotope Effects On Enzyme Catalyzed Reactions*; Cleland, W. W., O'Leary, M. H., Northrop, D. B., Eds.; University Park Press: Baltimore, 1977; pp 122−148.
(15) Miwa, G. T.; Garland, W. A.; Hodshon, B. J.; Lu, A. Y.; Northrop, D. B. *J. Biol. Chem.* **1980**, *255*, 6049−6054.
(16) Northrop, D. B. *Ann. Rev. Biochem.* **1981**, *50*, 103−131.
(17) Northrop, D. B. *Biochemistry* **1981**, *20* 4056−4061.
(18) Iyer, K. R.; Jones, J. P.; Darbyshire, J. F.; Trager, W. F. *Biochemistry* **1997**, *35*, 7136−7143.
(19) Jones, J. P.; Rettie, A. E.; Trager, W. F. *J. Med. Chem.* **1990**, *33*, 1242−1246.
(20) Kharki, S. B.; Dinnocenzo, J. P.; Jones, J. P.; Korzekwa, K. R. *J. Am. Chem. Soc.* **1995**, *117*, 3657−3664.
(21) The carbon atoms of the methyl groups are taken as the frame of reference for defining inter-methyl group distance (calculated using Spartan Molecular Mechanics software) since it is fixed, unlike the distances between the rotationally mobile inter-methyl group hydrogens. The distance of closest approach that can be achieved between two hydrogens that are bonded to different methyl groups in the same substrate is approximately 1.4 Å for *o*-xylene, 6.7 Å for *p*-xylene, and 11.1 Å for 4,4′-dimethylbiphenyl.
(22) Brown, F. K.; Kollman, P. A. *J. Mol. Biol.* **1987**, *198*, 533−546.
(23) MacKerell, A. D.; Nilsson, L.; Rigler, R.; Heinemann, U.; Saenger, W. *Proteins* **1989**, *6*, 20−31.
(24) Makinen, M. W.; Troyer, J. M.; van der Werff, H.; Bernedsen, H. J. C.; van Gunsteren, W. F. *J. Mol. Biol.* **1989**, *207*, 201−216.
(25) Collins, J. R.; Loew, G. H. *J. Biol. Chem.* **1987**, *263*, 3164−3170.
(26) Paulsen, M. D.; Bass, M. B.; Ornstein, R. L. *J. Biomol. Struct. Dyn.* **1991**, *9*, 187−203.
(27) Paulsen, M. D.; Ornstein, R. L. *J. Comp.-Aided Mol. Des.* **1992**, *6*, 449−460.
(28) Bass, B. B.; Paulsen, M. D.; Ornstein, R. L. *Proteins* **1992**, *13*, 26−37.
(29) Collins, J. R.; Camper, D. L.; Loew, G. H. *J. Am. Chem. Soc.* **1991**, *113*, 2736−2743.
(30) Jones, J. P.; Trager, W. F.; Carlson, T. J. *J. Am. Chem. Soc.* **1993**, *115*, 381−387.
(31) Jones, J. P.; Shou, M.; Korzekwa, K. R. *Biochemistry* **1995**, *34*, 6956−6961.

Table 1. Heat of Formation (ΔH_f), Relative Energies[a] of Radical from UHF AM1 Calculations and Relative Probability of Radical Formation

position and radical type[b]	relative stability (Kcal/mol)	relative probability of radical formation[c]
C3 (2^0)	1.65	0.063
C4 (3^0)	16.26	0.000
C5 (2^0)	0.04	0.932
C6 (2^0)	0.00	1.000
C1 (3^0)	18.03	0.000
C7 (2^0)	4.49	0.001

[a] Energies relative to the most stable radical. [b] The term (2^0) indicates a secondary radical center, and the term (3^0) indicates a tertiary radical center. [c] Calculated by eq 2.

Table 2. Predicted Percentage of Regio- and Stereoselectivity of Hydroxylation of D-(1*R*)- and L-(1*S*)-Norcamphor by P450 101 from Analysis of Steric Factors

position and stereochemistry	D-(1*R*)- norcamphor[a]	L-(1*S*)- norcamphor
C3-exo	1.2	1.6
C3-endo	0.2	0.0
C4	53.7	45.1
C5-exo	12.1	15.3
C5-endo	14.2	0.6
C6-exo	14.5	13.9
C6-endo	0.1	0.0
C1	0.0	0.0
C7-exo	2.7	22.2
C7-endo	1.4	1.3

[a] Regioselectivities were calculated from the distance and angle of a given hydrogen from the perferryl oxygen as described in Experimental Section.

energies for each carbon site were calculated from the heat of radical formation at each site. The results indicated that the rank order of energetically preferred radicals was C5 > C6 > C3 > C7 > C4 > C1. The relative stability values were then used to calculate the relative probability of specific radical formation. The results of this calculation are presented in Table 1, and are used as electronic criteria in predicting the regioselectivity of norcamphor hydroxylation. Because of the lower energies associated with radical formation at C3, C5, and C6, oxidation at these sites was deemed to be favored, whereas radical formation at C1, C4, or C7 was excluded because of the higher energies associated with these sites. Although the assumption that only these three carbons can form radicals is arbitrary, it is similar to the assumptions made by others.[32,33]

The Cartesian coordinates for the perferryl oxygen−substrate complex that were stored during the molecular dynamic runs were analyzed, using the steric criteria defined above, to establish which hydrogens on D-(1*R*)- or L-(1*S*)-norcamphor were oriented for catalysis. The results of this analysis are summarized in Table 2, and are expressed as a percentage. Hydroxylation is predicted to preferentially occur at carbon C4, (>45%), but with substantial additional oxidation at C5 (>15%) and C6 (>13%), for both enantiomers. Considerable hydroxylation was also predicted at C7 (>22%), but only for L-(1*S*)-norcamphor. Stereoselectivity of hydroxylation was confined to the exo position with one notable exception, the C5-endo position of D-(1*R*)-norcamphor. The C3-endo, C6-endo, and C1 hydrogen do not meet the defined steric criteria necessary for catalysis.

The steric predictions minus the potential sites of oxidation excluded by electronic effects are summarized in Table 3. The instability of the C4 radical signaled by the electronic component precludes its formation. Thus, hydroxylation is predicted to be confined to the C3, C5, and C6 sites for both stereoisomers. Stereoselectivity of hydroxylation is essentially exo for all L-(1*S*)-norcamphor carbon positions. However, in the case of D-(1*R*)-norcamphor, although reaction at the C6 and C3 positions is predicted to be exo, hydroxylation of C5 is predicted to be nonstereoselective. The experimentally determined percent regioselectivity values of the P450 101 catalyzed hydroxylation of D-(*R*)- and L-(*S*)-norcamphor[33] are tabulated together with the computationally derived values from the present study and those of Loida et al.[33] and Harris and Lowe[32] in Table 4.

Table 3. Predicted Percentage of Regio- and Stereoselectivity of Hydroxylation of D-(1*R*)- and L-(1*S*)-Norcamphor by P450 101 based on Analysis of Steric Factors at Those Sites not Excluded by Electronic Effects

position and stereochemistry	D-(1*R*)-norcamphor[a]	L-(1*S*)-norcamphor
C3-exo	0.2	0.3
C3-endo	0.0	0.0
C5-exo	28.6	49.4
C5-endo	33.9	2.0
C6-exo	37.0	48.3
C6-endo	0.3	0.0

[a] Regioselectivities were calculated from the distance and angle of a given hydrogen from the perferryl oxygen as described in Experimental Section.

Table 4. Experimental and Theoretical Regioselectivity (as percent) for the P450 101 Catalyzed Hydroxylation of D-(1*R*)- and L-(1*S*)-Norcamphor

	experiment[a]		Audergon		Loida[a]		Harris[b]	
position	D-(*R*)	L-(*S*)	D-(*R*)	L-(*S*)	D-(*R*)	L-(*S*)	D-(*R*)	L-(*S*)
C5	65	28	62.5	51.4	54	39	75.0	43.3
C6	30	62	37.3	48.3	41	57	18.7	38.9
C3	5	10	0.2	0.3	4	3	6.3	17.7

[a] Taken from Loida et al.33 [b] Taken from Harris and Loew.[32]

Table 5. Statistically Corrected Kinetic Isotope Effects for the Hydroxylation of the α-Methyl Group of *o*-Xylene, *p*-Xylene and 4,4′-Dimethylbiphenyl

substrate	isotope effect[a]
o-xylene-α-$^2H_1$-α′-$^2H_1$	8.4 ± 0.42 (3)[b]
o-xylene-α-$^2H_2$-α′-$^2H_2$	8.1 ± 0.29 (3)
o-xylene-α-$^2H_3$	10.6 ± 0.41 (3)
p-xylene-α-$^2H_1$-α′-$^2H_1$	7.5 ± 0.38 (6)
p-xylene-α-$^2H_2$-α′-$^2H_2$	7.4 ± 0.07 (6)
p-xylene-α-$^2H_3$	7.4 ± 0.37 (6)
4-$^2H_1$,4′-$^2H_1$-dimethylbiphenyl	5.5 ± 0.53 (6)
4-$^2H_2$,4′-$^2H_2$-dimethylbiphenyl	6.2 ± 0.15 (6)
4-$^2H_3$,4′-dimethylbiphenyl	2.7 ± 0.11 (6)

[a] Numerical value of the isotope effect plus or minus the standard deviation. [b] Number in parentheses is the number of determinations.

Isotope Effects for the Isomer Xylenes and 4,4′-Dimethylbiphenyl. The observed deuterium isotope effects for selectively deuterated xylene isomers and 4,4′-dimethylbiphenyl are listed in Table 5. With *o*-xylene and *p*-xylene, the observed isotope effect for the α-$^2H_3$-substrates were 10.6 and 7.4, respectively, and are similar to the observed isotope effect values for α-$^2H_1$-α′-$^2H_1$ and α-$^2H_2$-α′-$^2H_2$-deuterated substrates (8.4 and 8.1; 7.4 and 7.37, respectively). In the case of 4-$^2H_3$,4′-dimethylbiphenyl the observed isotope effect (2.7) is significantly smaller than the observed isotope effect (5.5 and 6.2) for the di- and tetradeuterated substrates, respectively.

Molecular Dynamics of Isomeric Xylenes and 4,4′-Dimethylbiphenyl. The results of the molecular dynamics simulations

(32) Harris, D.; Loew, G. *J. Am. Chem. Soc.* **1995**, *117*, 2738−2746.
(33) Loida, P. J.; Sligar, S. G.; Paulsen, M. D.; Arnold, G. E.; Ornstein, R. L. *J. Biol. Chem.* **1995**, *270*, 5325−5330.

Table 6. Number of Switches between Methyl Group and a Reactive Orientation during the Course of a Molecular Dynamics Run

substrate	distance between methyl group carbon atoms (Å)	number of switches in 1 ns molecular dynamics
o-xylene	2.48	1172[a]
m-xylene	5.0	779[b]
p-xylene	6.62	3
4,4′-dimethylbiphenyl	11.05	0

[a] Calculated from 500 ps of molecular dynamics. [b] Although no experimental results were obtained for *m*-xylene due to analytical complications, the theoretical data is worthy of consideration since it shows good correlation with the other isomers.

are shown in Table 6. As indicated in the methods section the simulations for *o*-xylene were conducted for 500 ps, whereas those for the other substrates were run for 1 ns. The predicted number of equilibration events, or switches, between the methyl groups were 1172, 779, 3, and 0 for *o*-xylene, *m*-xylene, *p*-xylene, and 4,4′-dimethylbiphenyl, respectively, when normalized to a 1-ns time span.

Discussion

In the earlier experimental paper on the isotope effects associated with the P450 catalyzed methyl group hydroxylation of *o*- and *p*-xylene and 4,4′-dimethylbiphenyl, the magnitudes of the observed isotope effects were found to decrease as the distance between reaction sites increased.[18] The results of these experiments support the hypothesis that the degree of masking of an intrinsic isotope effect in an intramolecular isotope effect experiment is directly related to the distance between equivalent but isotopically distinct methyl groups. Intuitively the relationship is appealing. One would certainly expect that the rate of equilibration of two methyl groups, with respect to a defined point in space, would decrease as the distance between the two methyl groups increased, particularly if any steric impediments (active-site topography) began to assume importance. A primary goal of this study was to carry out both computational and additional experimental studies that would further test this hypothesis, using the same set of substrates (isomeric xylenes and 4,4′-dimethylbiphenyl) but with an enzyme, P450 101, with known active site dimensions. If successful, these studies would also reinforce the notion that P450 101 can serve as a useful model for the mammalian P450s. Since the active-site structures of mammalian P450 are unknown, in computero studies based on the known crystal structures of several soluble cytosolic bacterial P450s might be used to predict and gain an understanding of mammalian P450s, provided they can be validated. Indeed, this is often the only way such information can be obtained. Thus, the validation of computational methods is extremely important toward evaluating the potential of the predictive power of this method.

Prior to determining whether molecular dynamic simulations of the motion of the isomeric xylenes and 4,4′-dimethylbiphenyl substrates in the active site of P450 101 were predictive of distance-dependent masking effects, our working model of the active enzyme needed to be validated. To this end D-(1*R*)- and L-(1*S*)-norcamphor were chosen as probe substrates. An X-ray crystal structure of D-norcamphor-P450 101 substrate−enzyme complex (7cpp.pdb) was available, and both computational and experimental results describing the P450 101 catalyzed hydroxylation of the racemic and enantiomeric forms of norcamphor were also available.[32−34] Moreover, predicting the P450 101 catalyzed hydroxylation of these substrates by computer simulation is particularly challenging because multiple products are formed. For example, an enantiomeric mixture of norcamphor metabolized by P40 101 results in the formation of 45% 5-*exo*-hydroxy-, 47% 6-exo-hydroxy-, and 8% 3-exo-hydroxynorcamphor,[34] while the 5-, 6-, and 3-hydroxy products are obtained in a ratio 65:30:5, respectively, from enantiomerically pure D-(1*R*)-norcamphor and in a ratio of 28:62:10, respectively, from enantiomerically pure L-(1*S*)-norcamphor.[33]

In this study the predicted regioselective results obtained for the formation of the 5-, 6-, and 3-hydroxy products from D-(1*R*)-norcamphor gave a ratio of 62.5:37.3:0.2, whereas those from L-(1*S*)-norcamphor gave a ratio of 51.4:48.3:0.3 for the corresponding products. Although not exact, these values are in reasonable accord with the experimental results for the individual enantiomers,[33] Table 4. However, evaluation of the predicted product stereoselectivities (exo versus endo, Table 3) are complicated by the fact that experimental product stereoselectivities have only been reported for racemic norcamphor[34] and not for the pure enantiomers.[33] The predicted product stereoselectivity for L-(1*S*)-norcamphor hydroxylation was predominantly exo at all carbon sites. This is also the major stereochemistry predicted for product formation at the C6 and C3 positions of D-(1*R*)-norcamphor. All of these results are in agreement with experiment and previously reported theoretical results,[32,33] Table 4. However, a major difference arises for the 5-hydroxylation of D-(1*R*)-norcamphor where our method predicts an exo/endo ratio of 0.85:1, Table 3. Although no experimental studies have appeared reporting the exo to endo product distribution for this enantiomer, these results would appear not to agree with the experimental results reported for the racemic mixture.[34]

Overall, the initial molecular dynamics simulations of the enzyme−substrate complex of P450 101 with D-(1*R*)- and L-(1*S*)-norcamphor incorporating only the motion of residues within 13 Å of the heme iron, and using a combination of steric and electronic criteria for analysis, gave good correlation with previously published values for the regio- and stereoselective hydroxylation of the norcamphor enantiomers by P450 101. It was therefore concluded that our methodology could serve as an appropriate model for testing the distance hypothesis.

The low energy barrier associated with rotation ensures that the rate of methyl group rotation is much faster than the rate of methyl group oxidation. If a substrate has a methyl group that is oxidized and the methyl group contains deuterium and protium, the enzyme has the choice of oxidizing either a C−H or a C−D bond. Since the rate of methyl group rotation is fast relative to oxidation, $(k_H/k_D)_{obs}$ will closely approach k_H/k_D. Thus, the observed intramolecular isotope effects for P450 101 catalyzed benzylic hydroxylation of the di- and tetradeuterated substrates studied here can be expected to closely approach the intrinsic isotope effects.[18] All values of $(k_H/k_D)_{obs}$ for these substrates are large and fall within a range of 5.5 to 8.4, (Table 5). The values of $(k_H/k_D)_{obs}$ for the trideuteromethyl xylenes are equally large, suggesting that within the active site of P450 101 even methyl group interchange is fast enough to effectively unmask the intrinsic isotope effect. In contrast, $(k_H/k_D)_{obs}$ for 4-$^2H_3$,4′-dimethylbiphenyl is only 2.7, suggesting that k_H/k_D for this substrate is highly masked. These results mirror the trends that were observed with these same substrates when either rat liver microsomes or purified P450 2B1 was used as the source of P450[18] and are consistent with the hypothesis that the extent of k_H/k_D masking increases with increasing distance between the catalytically susceptible methyl groups. For P450 101, just

(34) Atkins, W. M.; Silgar, S. G. *Biochemistry* **1988**, *27*, 1610−1616.

Scheme 1. Kinetic Scheme for Binding Substrate to Enzyme for an Intramolecular Isotope Effect Experiment with the Representative ES Complexes for *p*-xylene.

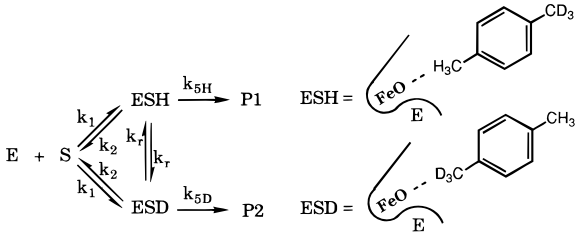

as for P450 2B1, the 11.05 Å separating the 4 and 4′ methyl groups of dimethylbiphenyl substrate is sufficiently large to prevent equilibration of these two groups with respect to the catalytically active oxygen in the time frame of the hydrogen atom abstraction.

The results of the molecular dynamics simulations are shown in Table 6. As described in the Experimental Section the simulations for *o*-xylene were conducted for 500 ps whereas those for the other substrates were run for 1 ns. In general, the aromatic rings remain perpendicular to the iron−oxygen bond during the course of the dynamics simulations for each substrate. The main motion of the molecules is a translational motion which allows each methyl group to approach the active-oxygen species. Thus, the molecule swings back and forth, placing first one than the other methyl group in position for oxidation. In the initial analysis of the run, the distance of every hydrogen atom of the substrate from the iron−oxygen bond was determined. Since the aromatic ring adopted an orientation coplanar to the heme, the average calculated distances from the oxygen atom were the smallest for the aromatic hydrogen. However, previously published experimental studies with the substrates used in this investigation together with several additional metabolic studies[35−37] indicate that the major metabolic pathway for substituted toluene is benzylic hydroxylation. Benzylic hydroxylation accounts for greater than 90% of the metabolic turnover of these substrates. We therefore did not include aromatic hydrogen in our molecular dynamics simulations and only considered the distances of the iron−oxygen from the methyl hydrogen.

The number of interchanges between the methyl groups were 1172, 779, 3, and 0 for *o*-xylene, *m*-xylene, *p*-xylene, and 4,4′-dimethylbiphenyl, respectively, when normalized to 1 ns. The trend in the data is exactly what would be expected. As the distance between intramolecular methyl groups increases, the number of methyl group interchanges decreases, and the intramolecular isotope effect gets smaller. The relationship between the number of interchanges and the degree of masking is hyperbolic and is given by the equation for the expression of an intramolecular isotope effect,[10] eq 1. The kinetic scheme outlined in Scheme 1 describes the simplest scheme that accounts for our observations. The rate constants k_1 and k_2 are for the rates of binding and debinding of substrate to the enzyme to form either an enzyme−substrate complex that can lead to hydrogen atom abstraction (ESH) or to deuterium abstraction (ESD). The rate constants for hydrogen or deuterium atom abstraction are k_{5H} for hydrogen atom abstraction, and k_{5D} for deuterium abstraction. The rate constant k_r determines the rate of interchange of the two ES complexes, ESH and ESD, with the substrate remaining in the binding site of the enzyme. Steady-state analysis of the product ratio leads to the following equation for the observed isotope effect for Scheme 1.

$$\frac{d[P1]}{d[P2]} = \left(\frac{k_H}{k_D}\right)_{obs} = \frac{\left(\frac{k_{5H}}{k_{5D}}\right)(k_2 + 2k_r) + k_{5H}}{(k_2 + 2k_r) + k_{5H}} \qquad (1)$$

Evaluation of the limits of this equation indicates that fast rotation, $k_r \gg k_{5H}$, leads to the intrinsic isotope effect being observed. For compounds with slow rotation an intrinsic isotope effect can still be observed if $k_2 \gg k_{5H}$. However, as k_2 and k_r become slower than k_{5H} the observed isotope effect will tend towards 1. Thus, isotope effects that are less than the intrinsic isotope effect require that both of the rate constants k_r and k_2 be slow relative to, or of the same order of magnitude as, k_{5H}. This appears to be the case for 4,4′-dimethylbiphenyl which gives a small isotope effect relative to the intrinsic isotope effect for the trideutero substrate. Thus, the rate constant k_2 is likely to be slow or of the same order of magnitude as k_{5H} for these reactions.

In general, these observations indicate that for *o*-xylene, the rate of equilibration between the methyl and perdeuteromethyl groups in the P450 101 active site is very fast and thus should not contribute to any observable masking of the intrinsic isotope effect. The rate of equilibration between the methyl groups drops dramatically for *p*-xylene but is apparently still rapid enough, relative to bond breaking, to allow the observation of an isotope effect that is close in magnitude to the intrinsic isotope effect. In contrast, no switching and a masked isotope effect of 2.7 is observed for 4,4′-dimethylbiphenyl during the time course of the dynamics simulations. These results suggest that an intramolecular distance of 11.05 Å is large enough to slow methyl group interchange to an extent that is sufficient to extensively mask the intrinsic isotope effect. In fact, eq 1 allows the rotation rate to be zero and the isotope effect to still be slightly unmasked by k_2 being approximately equal in rate to k_{5h}.

Conclusions

Both the computational and experimental results obtained with P450 101 in this study are entirely consistent with the experimental results found in the previous study.[18] Together the two studies provide strong evidence in support of the hypothesis that the degree of intrinsic isotope effect masking is directly related to the distance between chemically equivalent but isotopically distinct intramolecular catalytic sites, i.e., the distance hypothesis. The results of the computational studies provide additional support for establishing computational analysis as a valid methodology for understanding and predicting protein/small molecule interactions. Several other investigators have also conducted similar parallel experimental and theoretical studies with P450 101 and successfully predicted metabolite profiles, the salient examples being norcamphor,[33] *cis*-β-methylstyrene,[38] and nicotine.[30] However, to our knowledge this is he first example where the trend in masking an intrinsic isotope effect has been qualitatively predicted from molecular dynamics simulations.

Finally, an additional interesting feature to emerge from this study is the indication that it might be possible to synchronize the clock associated with defined conditions of molecular dynamics runs with relative methyl group interchange rates and the magnitude of the observed isotope effect. The most telling

(35) Hanzlik, R. P.; Hogberg, K.; Moon, J. B.; Judson, C. M. *J. Am. Chem. Soc.* **1985**, *107*, 7164−7167.
(36) Riley, P.; Hanzlik, R. P. *Xenobiotica* **1994**, *24*, 1−16.
(37) Higgins, L.; Bennett, G. A.; Shimoji, M.; Jones, J. P. *Biochemistry* **1998**, *37*, 7039−7046.
(38) Fruetel, J. A.; Collins, J. R.; Camper, D. L.; Loew, G. H.; Ortiz de Montellano, P. R. *J. Am. Chem. Soc.* **1992**, *114*, 6987−6993.

data in this regard are that collected for *p*-xylene. The observation of an intrinsic isotope effect for hydroxylation of this substrate requires that a number of interchanges must occur between the enzyme−substrate complexes prior to product formation. Three such interchanges are predicted to occur over a 1 ns molecular dynamics simulation. The fact that only three interchanges occur over the 1 ns of simulation, even though experimental observation indicates that the intrinsic isotope effect is completely unmasked, strongly suggests that shorter simulation times would be inadequate. On the other hand, the zero interchanges observed for 4,4′-dimethylbiphenyl over 1 ns of simulation, coupled to its extensively masked intrinsic isotope effect suggests that the rate of interchange will be sufficiently slow so that the effects of masking begin to become observable. Thus, it appears that longer simulations would be required to define a substrate that would have a partially masked isotope effect. While it is clear that simulation time cannot be directly related to wall clock time, these simulations and the conditions under which they were run provide a lower limit for the simulation time required to sample active site motion.

Experimental Section

Chemicals. *o*-Methyltoluate, *p*-methyltoluate, pentane, silica gel, dimethylphthalate, terephthalic acid, sodium borohydride, sodium borodeuteride, pthalic dicarboxaldehyde, terephthaldehyde, 4,4′-dimethylbiphenyl chromium trioxide, and Diazald were obtained from Aldrich Chemical Co., and lithium aluminum deuteride and lithium aluminum hydride were obtained from Fluka. Organic solvents were purchased from J.T. Baker and were of analytical grade. *N*-methyl-*N*-(*tert*-butyldimethylsilyl) trifluoroacetamide (MTBSTFA) was purchased from Pierce, and *p*-toluenesulfonyl chloride was obtained from Eastman Kodak. Biochemicals were obtained from Sigma.

Synthesis of Substrates. Selectively deuterated xylene isomers and 4,4′-dimethylbiphenyl, *o*-xylene-α-$^2H_3$, *p*-xylene-α-$^2H_3$, 4-$^2H_3$,4′-dimethylbiphenyl, *o*-xylene-α-$^2H_2$-α′-$^2H_2$, *p*-xylene-α-$^2H_2$-α′-$^2H_2$, 4-$^2H_2$,4′-$^2H_2$-dimethylbiphenyl, *o*-α-$^2H_1$-α′-$^2H_1$, *p*-xylene-α-$^2H_1$-α′-$^2H_1$, 4-$^2H_1$,4′-$^2H_1$-dimethylbiphenyl were synthesized as was described previously.[18]

Enzyme Preparation. *Pseudomonas putida* was grown according to literature procedure.[39] The cell free lysate that contained P450 101 was stored frozen in a saturated solution of camphor. The camphor was removed just prior to use by eluting the solution through a Sephadex G-15 column with 50 mM potassium phosphate buffer, pH 7.

Incubation Conditions. An aliquot of camphor-free phosphate buffer from the Sephadex G-15 column eluant described above, sufficient to contain 10 nmol of P450 101,[40] was added to each incubation vial, along with NADH, 12.3 μmol, and substrate (xylenes 4.08 mM and 4,4′-dimethylbiphenyl 0.67 mM) in a total volume of 2 mL of 50 mM potassium phosphate buffer, pH 7. Incubations were run for 30 min at 27 °C then terminated by the addition of 5 mL of pentane and stored at −78 °C until analysis.

Derivatization and Analysis by GC/MS. The frozen incubation mixtures were thawed, and the aqueous layer was extracted with 2 × 5 mL portions of pentane. The pentane layers were pooled, dried over sodium sulfate, and concentrated under a stream of nitrogen gas to 30 μL. The samples were derivatized with 150 μL of 60% MTBSTFA in acetonitrile at 65 °C for 3 h and analyzed by GC/MS. GC/MS analysis was performed on a VG7070 mass spectrometer, interfaced to a HP-5710A GC fitted with a 15 m J & W DB-5 fused silica capillary column and operated in the selected ion-monitoring mode. The derivatized xylenes were cold trapped at 40 °C, the temperature was raised linearly at 15 °C/min to 135 °C followed by isothermal elution for 5 min. For the derivatized biphenyls an initial temperature of 100 °C for 1 min followed by a linear ramp at 15 °C/min to 250 °C followed by isothermal elution for 5 min was used. The $[M - 57]^+$ ion of the silyl derivative was monitored for the various xylene isomer metabolites and 4,4′-dimethylbiphenyl metabolites. Mass spectral conditions were as follows: 50 ms dwell time, −70 eV ionizing voltage, and 200−205 °C source temperature.

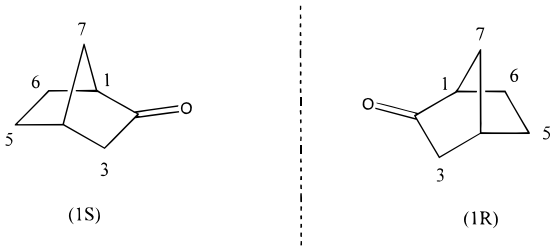

Figure 2. The structures and carbon framework numbering system of L-(1*S*)- and D-(1*R*)-norcamphor.

The deuterium incorporation of each substrate was determined by using the same GC parameters as those used for the respective metabolites or by bleeding the compound through the reference inlet. The mass spectral conditions were identical to those used for the metabolites except that the ionizing voltage was −12.5 eV. The measured ion intensity of each ion was corrected for the natural isotopic abundance of ^2H, ^{13}C, ^{14}C, ^{18}O, and ^{29}Si,[41] and isotope effects were determined as described previously.[10,12]

Computational Methodology

A. Validation of the Model with D-(1*R*)- and L-(1*S*)-Norcamphor. A detailed description of the methods is given by Jones and Korzekwa.[42] The semi-empirical quantum chemical Austin method (AM1), as provided in the MOPAC 6.0 programs was used to calculate the minimized geometry, the charges, and the heat of formation of all the molecules. The unrestricted Hartree−Fock (UHF) Hamiltonian was used for all open-shell calculations (radicals). The protoporphyrin parameters were developed, with an oxygen bound to the iron 1.7 Å above the heme, as previously reported.[30] Briefly, the coordinates of the heme−iron−sulfur complex were obtained from the crystal structure of P450 101 with substrate bound (Brookhaven data bank, 2cpp.pdb). The full porphyrin complex was used including all of the side chains and the anionic forms of the propionate groups. The cysteine residue was replaced with a thiomethane anion and the methyl group oriented in a configuration similar to that of the methylene group of cysteine. The charges were determined with the Gaussian 90 ab initio package, the LANL1MB basis set. Natural population analysis was done by the method of Reed and Weinhold.[43]

Molecular dynamic simulations were performed using the AMBER 4.0 suite of programs. The Cartesian coordinations for all of the atoms except the ferryl oxygen and hydrogen atoms used for the initial D-(1*R*)-norcamphor complex with P450 101 were obtained from the X-ray crystal structure of D-(1*R*)-norcamphor bound to P450 101 (Brookhaven data bank, 7cpp.pdb). In the case of L-(1*S*)-norcamphor the substrate was docked in a configuration similar to that of D-(1*R*)-norcamphor, by overlaying the oxygen atoms and the C2 carbons and orienting C1 close to C3, Figure 2.

The belly option was used to limit the dynamic motion to the substrate and the 53 amino acids located within a radius of 13 Å above the heme iron, forming an hemisphere representing the "belly". All calculations were performed with a nonbonded cut-off distance of 8 Å, and the nonbonded pair list was updated every 0.1 ps. A constant dielectric function was used for electrostatic calculations. The energy of the entire system was minimized with 1500 steps of steepest descent followed by a conjugated gradient minimization until the convergence gradient for either energy (2 cal/mol) or norm of gradient energy (2 cal/mol/Å) was reached. The system was warmed and stabilized in three stages of 10 ps each at 100 K, 200 K, and 300 K, respectively.

(39) Gunsalus, I. C.; Wagner, G. C. *Methods Enzymol.* **1978**, *52*, 166−188.

(40) Omura, T.; Sato, R. *J. Biol. Chem.* **1964**, *239*, 2370−2378.

(41) Korzekwa, K. R.; Howald, W. N.; Trager, W. F. *Biomed. Environ. Mass Spectrom.* **1990**, *19*, 211−217.

(42) Jones, J. P.; Korzekwa, K. R. *Methods Enzymol.* **1996**, *272*, 326−335.

(43) Reed, A. E.; Weinstock, R. B.; Weinhold, F. *J. Chem. Phys.* **1985**, *83*, 735−746.

Simulations were performed over 500 ps on each enantiomer at 300 K, and the Cartesian coordinates of each atom in the enzyme−substrate complex were stored every 0.1 ps. A constant temperature for the simulation was maintained by weakly coupling a thermal bath with a 0.1-ps strength constant. The rms changes in total energy and temperature stabilized at less then 13.6 Kcal/mol and 6.0 K respectively, indicating that the system was reasonably equilibrated.

Molecular dynamic simulations were analyzed using the Tripos Associates SYBYL program. Previous publications have used the substrate hydrogen−ferryl oxygen distance and the corresponding carbon−hydrogen−ferryl oxygen angle as defining steric criteria for establishing when a given hydrogen's position has reactive geometry.[32,33] These two criteria were applied simultaneously to the simulation results to define the reactivity of each of the various hydrogens; (1) the hydrogen atom on a specific carbon atom had to be close enough to the ferryl oxygen atom to be abstracted (less than 3.5 Å), and (2) the angle defined by the ferryl oxygen, hydrogen, and carbon (O−H−C) had to be linear with a deviation less than ±70°. Only one reactive position is allowed at one time. If more than one site meets the above steric criteria, an electronic criterion is invoked to select the reactive position. The electronic criterion is based on the relative stability of the radical intermediates (see below). Finally, if two hydrogens from the same carbon are potentially reactive, the one nearest to the ferryl oxygen atom is chosen.

The relative radical energies for each carbon site were calculated from the heat of formation of the radicals. This method had previously been used by Harris and Loew[32] in the assessment of the relative stability of primary, secondary, and tertiary radicals. The relative probability of radical formation was calculated using eq 2, and represents the electronic reactivity of a given carbon site.

$$n1/n2 = \exp(\Delta\Delta H_f/RT) \qquad (2)$$

where $\Delta\Delta H_f$ is equal to the relative radical stability shown in Table 1 at sites $n1$ and $n2$, R the gas constant (0.001987 Kcal/deg mol]), and T the absolute temperature in degrees kelvin (K). Finally, the contribution of the steric and electronic reactivity factors are used to predict the regio- and stereospecificity of D-(1*R*)- and L-(1*S*)-norcamphor hydroxylation.

B. Molecular Dynamics of Isomeric Xylenes and 4,4′-Dimethylbiphenyl. The molecular dynamics of the isomeric xylenes and 4,4′-dimethylbiphenyl were studied by using the protocols established above. Numerous initial docking positions were tested for *p*-xylene in the active site of P450 cam. However, after 10 ps of molecular dynamics, all of the initial docking positions converged to approximately the same location within the active site. This location, in which *p*-xylene is oriented for catalysis, was then used as a starting position for molecular dynamics calculations. Subsequently, it was also used as a template to locate the starting positions for *o*-xylene, *m*-xylene, and 4,4′-dimethylbiphenyl.

To obtain a reasonable sample of the possible conformational space available to the various substrates, dynamic simulations were performed for 500 ps for *o*-xylene but extended to 1 ns for *m*-xylene, *p*-xylene, and 4,4′-dimethylbiphenyl. For the same reason, molecular dynamics studies were conducted at 600 K instead of 300 K. The final run temperature of 600 K was reached by warming each system in 4 stages of 10 ps each (100 K, 200 K, 300 K, and 600 K). The rms changes in total energy and temperature for all of the molecules were similarly stabilized at less than 16.9 Kcal/mol and 11.6 K, respectively, indicating that the systems were reasonably equilibrated.

The distance between each benzylic hydrogen and the perferryl oxygen was measured. The interchange, or switching, between the two methyl groups with respect to the perferryl oxygen was defined by the following criteria: (1) how often a hydrogen atom from a given methyl group that is poised for catalysis (within 3.5 Å of the perferryl oxygen) is replaced by a hydrogen from the alternate methyl group within the time allocated (up to 1 nsec) and (2) when the selected hydrogen forms a carbon−hydrogen−oxygen angle that deviates less than ±70° from linearity.

Acknowledgements. This research was supported in part by the National Institutes of Health (Grants ES 09122 (J.P.J.) and GM 36922 (W.F.T.) and in part by the Swiss National Science Foundation (C.A.). We also thank the reviewer who suggested that we present eq 1 and Scheme 1 to describe our results and Ken Korzekwa for his helpful comments.

JA983000W